

Initial measurement of electron nonextensive parameter with electric probe

Huibin Qiu,^{*} Zhenyu Zhou,[†] Xingkun Peng,[†] Xianyang Zhang,[†] Yuqing Zhu,[†] Yue Gao,[†] Donghua Xiao,[†] Haifeng Bao, Tianling Xu, Jia Zhang, Tianhui Huang, Jinmao Zhou, Zhiyi Ming, Pengfei Xiang, Hai Yang, Xiaofeng Wang, Dongyang Wu, and NCST Team

*Department of Physics, Nanchang University, Jiangxi, Nanchang 330031, China
and Jiangxi Province Key Laboratory of Fusion and Information Control, Nanchang University, Jiangxi, Nanchang 330031, China*



(Received 21 January 2020; revised manuscript received 16 March 2020; accepted 16 March 2020; published 16 April 2020)

Theoretical analysis and a large number of experiments have proved that plasma components do not satisfy Boltzmann-Gibbs statistics and can be well described by nonextensive statistical mechanics, while new plasma parameters, electron nonextensive parameters, which are introduced to describe the nonextensive properties of plasma, cannot be diagnosed yet. Here we show measurement of electron nonextensive parameters of plasma with a *nonextensive* single electric probe. Our results show that nonextensive electric probe may play a role in plasma diagnosis, measuring nonextensivity of plasma and improving diagnostic accuracy of other plasma parameters. We expect the proposed *nonextensive* single electric probe can be starting point of more complex nonextensive electric probe. In addition, nonextensive electric probe is an important means to study various plasma waves and instability, turbulence, and anomalous transport, and a definite and quantitative test of the theory of nonextensive geodetic acoustic models will be relevant to such development.

DOI: [10.1103/PhysRevE.101.043206](https://doi.org/10.1103/PhysRevE.101.043206)

I. INTRODUCTION

In the field of plasma parameter diagnosis, much of plasma parameter information is obtained by electric probe diagnosis [1]. Presupposition distribution of components in plasma is very important for single probe measurement, which requires the presupposition of which statistical mechanics can be used to describe the plasma to be measured [2,3]. Statistical hypothesis of plasma includes Boltzmann-Gibbs statistical mechanics, in which plasma components obey the Maxwellian distribution. However, theoretical analysis [4,5] and a large number of experiments [6–10] have proved that plasma components do not satisfy Boltzmann-Gibbs statistics and can be well described by nonextensive statistical mechanics [11–13], while the new plasma parameters, electron nonextensive parameters, which are introduced to describe the nonextensive properties of plasma, cannot be diagnosed yet. Here we show the measurement of electron nonextensive parameters of plasma with a *nonextensive* single electric probe. We assume that the plasma to be measured can be described by nonextensive statistical mechanics and then establish nonextensive single electric probe theory. Using nonextensive single electric probe, we measured an electron nonextensive parameter of 0.775 (see Table I) that cannot be measured by a traditional single probe and obtained more accurate electron temperature, plasma potential, electron density, and floating potential than a traditional single probe. Our results show that nonextensive electric probe may play a role in plasma diagnosis, measuring the nonextensivity of

plasma, and improving diagnostic accuracy of other plasma parameters. We expect that the proposed nonextensive single electric probe can be the starting point of more complex nonextensive electric probes. For example, it is possible to develop nonextensive single electric probes including effects of magnetic field, collision, secondary electron emission, rf field, etc., as well as nonextensive double, triple, four, five, or N electric probes and an array of nonextensive electric probes. In addition, nonextensive electric probe is an important means to study various plasma waves and instability, turbulence, and anomalous transport, and a definite and quantitative test of nonextensive geodetic acoustic models theory [14] will be relevant to such development.

Nonextensive single electric probe is a small solid conductor (there are various sizes and shapes; the most common shapes are spherical, cylindrical, and flat; it is usually made from materials such as molybdenum, tungsten, and graphite, while for chemically active plasmas it is platinum and gold; the probe holder can be made of glass, quartz, or ceramic material) that penetrates into the edge of a plasma to collect electron and ion flows and connected to the outside world (power supply, voltmeter, ammeter, etc.) through some kind of circuit (as shown in Fig. 1). By directly measuring the particle flux flowing to the surface of the probe, the information described by nonextensive statistical mechanics of the plasma measured by the probe (electron nonextensive parameters, electron temperature, plasma potential, electron density and floating potential, etc.) is derived; with simple structure and good spatial resolution, for diagnosis of low-temperature plasma or high-temperature plasma (parameters) in the boundary region of tokamak devices or in the divertor, it is an important means to study various plasma waves, instability, turbulence, and anomalous transport. Recent plasma studies [4,15–17]

*huibinqiu@ncu.edu.cn

[†]These authors contributed equally to this work.

TABLE I. Nonextensive single electric probe measurement results.

Plasma parameters	ESP formula	ESP fitting	NSP fitting
q_{Fe}	—	—	0.775
T_e (eV)	7.0497	6.8843	2.8358 ^a
Φ_p (V)	23.6083	24.7228	19.4528
n_e (10^{15}cm^{-3})	1.186	1.263	1.936
Φ_f (V)	0.070922	1.7377	2.0397
$\alpha_{q_{Fe}}$	—	3.3388	6.1405
SSE (arb. units)	594.0110	313.2270	303.9174
R^2	0.86765	0.93021	0.93229

^aA dash denotes no measured value.

have shown that plasma composition in the actual situation is not completely following the ideal Maxwellian distribution and always deviates from the Maxwellian distribution, which shows that the method for describing plasmas, namely statistical theory, requires innovation, or the way to describe plasma needs to change, such as plasma is regarded as composed of Maxwellian composition and non-Maxwellian composition. The latest research [17] tends to support the former approach: Experiments [6,7], theories [15,18], and simulations [4] show that even in equilibrium plasmas, the components do not always meet the ideal Maxwellian distribution. In addition, one candidate, nonextensive statistical mechanics, shows strong compatibility [17]: The distribution derived from it is uniform at time of $q_{Fe} \rightarrow -1$; κ distribution while $-1 < q_{Fe} < 1$ [19,20]; regressive to Maxwellian distribution at extensive limit ($q_{Fe} = 1$) [21]; truncated distribution, which has a cutoff in the tail when $q_{Fe} > 1$; and Dirac delta function at a limit of $q_{Fe} \rightarrow +\infty$, which shows that if nonextensive statistical mechanics is chosen to describe the plasma, it not only has the advantage of covering the results under the Boltzmann-Gibbs statistical mechanics framework and proving the correctness of the theory itself for the extensive limit but also has the advantage of obtaining the conclusion that can cover at least four other cases. Here we set up the theory of nonextensive single electric probe that can measure electron nonextensive parameters that the traditional electric probe cannot measure and improve the measuring accuracy of the single electric

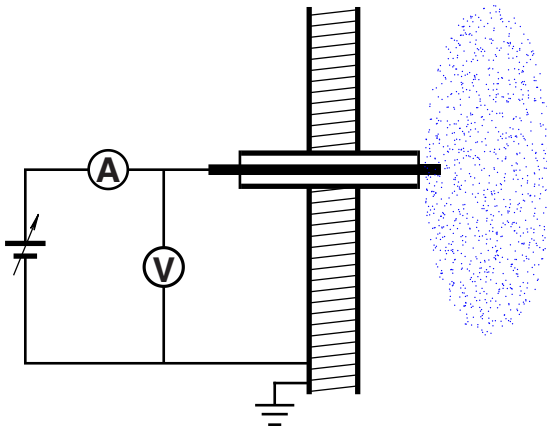


FIG. 1. Single electric probe diagram. For details see the supplementary information for the caption to Fig. 1 given in Appendix B.

probe by introducing nonextensive statistical mechanics to take into account the nonextensivity of systems that have been proved by a large number of facts (it may be caused by a long-range interaction effect).

II. THEORETICAL FOUNDATION OF NONEXTENSIVE SINGLE ELECTRIC PROBE

In order to obtain the nonextensive probe theory consistent with the experiment, we extend the electrostatic probe theory under the Boltzmann-Gibbs statistical framework to the theory under the nonextensive statistical framework. The obtained theoretical formula of single probe under nonextensive statistical framework is as follows (see Appendix A):

$$I = en_e A_p \sqrt{\frac{\kappa_B T_e}{m_i}} \left\{ \frac{A_q}{q_{Fe}} \sqrt{\frac{m_i}{2\pi m_e}} \times \left[1 + (q_{Fe} - 1) \frac{e(V - \Phi_p)}{\kappa_B T_e} \right]^{\frac{1}{q_{Fe}-1} + \frac{1}{2}} - \left[1 - (q_{Fe} - 1) \frac{1}{2} \right]^{\frac{1}{q_{Fe}-1} + \frac{1}{2}} \right\}, \quad (1)$$

when $V < \Phi_p - \kappa_B T_e / 2e$. The above formula is clearly illustrated in Fig. 2 and Table II as follows: It can be seen from Fig. 2(a) that the curves with different nonextensive parameters are different, and the curves do not have simple integral monotony with respect to electron nonextensive parameters; the saturation ion current increases with the increase of the electron nonextensive parameters [also see Fig. 2(b)], and the floating potential increases with the increase of the electron nonextensive parameters, too [also reflected in Fig. 2(c), because $\Phi_f = \Phi_p - \alpha_{q_{Fe}} T_e$], while the current collected by probe decreases with the increase of the electron nonextensive parameter when the bias voltage is the ion sheath potential [also see Fig. 2(d)]. This indicates that the single probe I - V curve, the theoretical cornerstone of single-probe diagnosis, has a complex dependence on the nonextensive parameters, which is different from the traditional electric probe theory without the nonextensive parameters; in addition, we find that the above results return to the traditional theory based on the Boltzmann-Gibbs statistical framework in the extensive limit, which proves the correctness and universality of the nonextensive theory (namely a larger scope of application).

III. PRACTICAL APPLICATION OF NONEXTENSIVE SINGLE ELECTRIC PROBE

The above analysis has shown that the nonextensive parameters have effects on the single probe I - V curves. So then what are the influences of the nonextensive parameters on the proposed nonextensive single electric probe based on the I - V curves? The quantities that can be measured by the traditional single probe theory are Φ_f , T_e , Φ_p , and n_e , while the proposed nonextensive single electric probe theory can not only measure the four quantities with higher precision but also measure the electron nonextensive parameters q_{Fe} that cannot be measured by the traditional electric probe.

A. Floating potential

Floating potential can be measured simply by taking out the probe signal at each bias voltage and using the following

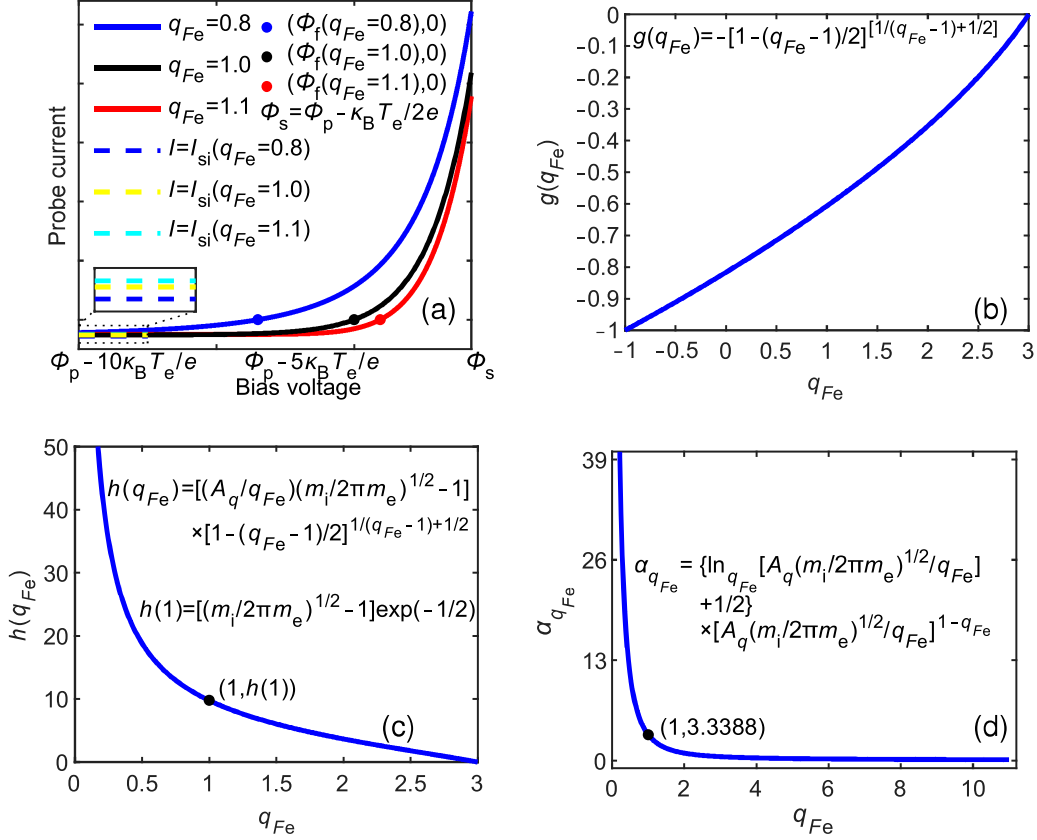


FIG. 2. Characteristics of the nonextensive single electric probe I - V curves. (a) Nonextensive single electric probe I - V characteristic curves show that current collected by probe monotonically increases with the increase of probe bias voltage. For cases of different nonextensive parameters, when the nonextensive parameter is 1, all conclusions return to the results under the Boltzmann-Gibbs statistical framework [17]; the current collected by probe has no integral monotone property with respect to the electron nonextensive parameter, and the local monotone property can be discussed in three derived graphs. (b) The dependence curve of ion saturation current factor on electron nonextensive parameter $[g(q_{Fe}) - q_{Fe}]$ shows that the ion saturation current factor has a monotonic increasing trend for nonextensive parameter. (c) The dependence curve of the total current factor on the electron nonextensive parameter ($I_s - q_{Fe}$) shows that the total current measured by a nonextensive single electric probe decreases monotonically with the increase of the electron nonextensive parameter. (d) The variation curve of the sheath potential coefficient measured with the nonextensive single electric probe with respect to electron nonextensive parameter ($\Phi_f - q_{Fe}$ is converted to $\alpha_{q_{Fe}} - q_{Fe}$) shows that sheath potential coefficient varies monotonically with the electron nonextensive parameter in the range we are interested in, namely the floating potential increases with the increase of the nonextensive electron parameter (for details see the supplementary information for the caption to Fig. 2 and Table II given in Appendix B).

equation:

$$\Phi_f = \sum_{|I_i| < \varepsilon} V_i / \text{card}(\{(V_i, I_i) \mid |I_i| < \varepsilon\}), \quad (2)$$

where ε is a small quantity that we choose. The floating potential measurement by this method is not affected by the nonextensive parameters; this method only uses the partial

TABLE II. Data presentation for curve of $\alpha_{q_{Fe}} - q_{Fe}$ and $\eta_{\alpha_{q_{Fe}}} - q_{Fe}$.

$\eta_{\alpha_{q_{Fe}}}$	$\alpha_{q_{Fe}} (0 < q_{Fe} < 1)$	$\alpha_{q_{Fe}} (q_{Fe} \geq 1)$	$q_{Fe} (0 < q_{Fe} < 1)$	$q_{Fe} (q_{Fe} \geq 1)$
$ \eta_{\alpha_{q_{Fe}}} \leq 5\%$	$3.3388 < \alpha_{q_{Fe}} \leq 3.5025$	$3.1694 \leq \alpha_{q_{Fe}} \leq 3.3388$	$0.974 \leq q_{Fe} < 1.000$	$1.000 \leq q_{Fe} \leq 1.029$
$5\% < \eta_{\alpha_{q_{Fe}}} \leq 10\%$	$3.5025 < \alpha_{q_{Fe}} \leq 3.6785$	$3.0022 \leq \alpha_{q_{Fe}} < 3.1694$	$0.948 \leq q_{Fe} < 0.974$	$1.029 < q_{Fe} \leq 1.060$
$10\% < \eta_{\alpha_{q_{Fe}}} \leq 15\%$	$3.6785 < \alpha_{q_{Fe}} \leq 3.8379$	$2.8385 \leq \alpha_{q_{Fe}} < 3.0022$	$0.926 \leq q_{Fe} < 0.948$	$1.060 < q_{Fe} \leq 1.093$
$15\% < \eta_{\alpha_{q_{Fe}}} \leq 20\%$	$3.8379 < \alpha_{q_{Fe}} \leq 4.0079$	$2.6705 \leq \alpha_{q_{Fe}} < 2.8385$	$0.904 \leq q_{Fe} < 0.926$	$1.093 < q_{Fe} \leq 1.130$
$20\% < \eta_{\alpha_{q_{Fe}}} \leq 25\%$	$4.0079 < \alpha_{q_{Fe}} \leq 4.1723$	$2.5054 \leq \alpha_{q_{Fe}} < 2.6705$	$0.884 \leq q_{Fe} < 0.904$	$1.130 < q_{Fe} \leq 1.170$
$25\% < \eta_{\alpha_{q_{Fe}}} \leq 30\%$	$4.1723 < \alpha_{q_{Fe}} \leq 4.3379$	$2.3342 \leq \alpha_{q_{Fe}} < 2.5054$	$0.865 \leq q_{Fe} < 0.884$	$1.170 < q_{Fe} \leq 1.216$
$30\% < \eta_{\alpha_{q_{Fe}}} \leq 35\%$	$4.3379 < \alpha_{q_{Fe}} \leq 4.5040$	$2.1709 \leq \alpha_{q_{Fe}} < 2.3342$	$0.847 \leq q_{Fe} < 0.865$	$1.216 < q_{Fe} \leq 1.265$
$35\% < \eta_{\alpha_{q_{Fe}}} \leq 40\%$	$4.5040 < \alpha_{q_{Fe}} \leq 4.6797$	$2.0023 \leq \alpha_{q_{Fe}} < 2.1709$	$0.829 \leq q_{Fe} < 0.847$	$1.265 < q_{Fe} \leq 1.322$
$40\% < \eta_{\alpha_{q_{Fe}}} \leq 45\%$	$4.6797 < \alpha_{q_{Fe}} \leq 4.8444$	$1.8363 \leq \alpha_{q_{Fe}} < 2.0023$	$0.813 \leq q_{Fe} < 0.829$	$1.322 < q_{Fe} \leq 1.386$
$45\% < \eta_{\alpha_{q_{Fe}}} \leq 50\%$	$4.8444 < \alpha_{q_{Fe}} \leq 5.0179$	$1.6701 \leq \alpha_{q_{Fe}} < 1.8363$	$0.797 \leq q_{Fe} < 0.813$	$1.386 < q_{Fe} \leq 1.460$

TABLE III. Data presentation for curve of $\eta_{\text{sin},T_e} - q_{Fe}$ at $V - \Phi_p = -\kappa_B T_e / 2e$.

η_{sin,T_e}	$q_{Fe}(q_{Fe} < 1)$	$q_{Fe}(q_{Fe} \geq 1)$
$ \eta_{\text{sin},T_e} \leq 5\%$	$0.900 \leq q_{Fe} < 1.000$	$1.000 \leq q_{Fe} \leq 1.100$
$5\% < \eta_{\text{sin},T_e} \leq 10\%$	$0.800 \leq q_{Fe} < 0.900$	$1.100 < q_{Fe} \leq 1.200$
$10\% < \eta_{\text{sin},T_e} \leq 15\%$	$0.700 \leq q_{Fe} < 0.800$	$1.200 < q_{Fe} \leq 1.300$
$15\% < \eta_{\text{sin},T_e} \leq 20\%$	$0.600 \leq q_{Fe} < 0.700$	$1.300 < q_{Fe} \leq 1.400$
$20\% < \eta_{\text{sin},T_e} \leq 25\%$	$0.500 \leq q_{Fe} < 0.600$	$1.400 < q_{Fe} \leq 1.500$
$25\% < \eta_{\text{sin},T_e} \leq 30\%$	$0.400 \leq q_{Fe} < 0.500$	$1.500 < q_{Fe} \leq 1.600$
$30\% < \eta_{\text{sin},T_e} \leq 35\%$	$0.300 \leq q_{Fe} < 0.400$	$1.600 < q_{Fe} \leq 1.700$
$35\% < \eta_{\text{sin},T_e} \leq 40\%$	$0.200 \leq q_{Fe} < 0.300$	$1.700 < q_{Fe} \leq 1.800$
$40\% < \eta_{\text{sin},T_e} \leq 45\%$	$0.100 \leq q_{Fe} < 0.200$	$1.800 < q_{Fe} \leq 1.900$
$45\% < \eta_{\text{sin},T_e} \leq 50\%$	$0.000 \leq q_{Fe} < 0.100$	$1.900 < q_{Fe} \leq 2.000$

data near the zero value of current to calculate the floating potential in relative isolation, and the result only reflects the local characteristics of the experimental data but cannot reflect the overall characteristics of the data. The whole data fitting method (WDFM) can overcome this difficulty: Using WDFM, the floating potential measured by the traditional single probe is 1.7377 V, while the floating potential measured by the nonextensive single electric probe is 2.0397 V (see Table I). It can be seen that the floating potential measurement by WDFM is affected by the nonextensive parameters. Moreover, the measurement results of nonextensive single electric probe are better than those of traditional single probe, which can be seen from the fact that the goodness of fit of nonextensive single probe (sum of squares due to error) $SSE = 303.9174$ arb. units is less than that of traditional single probe $SSE = 313.2270$ arb. units (see Table I).

B. Electron temperature

In order to measure the plasma electron temperature, we first read the ion saturation current directly from the observed data: $I_{\text{si}} = \sum_{V_i < V_c} I_i / \text{card}(\{(V_i, I_i) | V_i < V_c\})$, where V_c is a judgment potential artificially selected, and here the selection method is as follows: $V_c = \Phi_s - 2(\Phi_s - \Phi_f) \simeq 2\Phi_f - \max\{V_i\}$. Note that when you take $\max\{V_i\}$, the data requests to have been processed, namely the data greater than the ion sheath potential, have been deleted; if it is the original data, then Φ_s can be estimated by direct observation or by the method of “semilog-knee” (note that taking the semilog is the value of the original data plus the absolute value of saturated ion current) [22]. Then the electron temperature can be measured by using the above theory in the framework of nonextensive statistics:

$$\frac{\kappa_B T_{e,\text{sin}}}{e} = \{d[\ln(I + I_{\text{si}})]/dV\}^{-1} - (q_{Fe} - 1)(V - \Phi_p). \quad (3)$$

It is noted that the Maxwellian plasma electron temperature $T_{e,\text{sin}}(q_{Fe} = 1)$ can be obtained by the above equation, which proves the correctness of the proposed theory of nonextensive single electric probe at extensive limit. At this point, it can be seen that for the more general nonextensive case, the temperature $T_{e,\text{sin}}(q_{Fe} \neq 1)$ cannot be directly obtained, because it depends on the value of the electron nonextensive parameter q_{Fe} and $(V - \Phi_p)$. However, we have $(V - \Phi_p) \lesssim -\kappa_B T_e / 2e$, which cannot be equal to 0. Therefore, the single-

probe method cannot eliminate the influence of nonextensive parameters on plasma electron temperature measurement, and the influence degree can be described by the following expression (method error):

$$\eta_{\text{sin},T_e} = \frac{(q_{Fe} - 1)(V - \Phi_p)}{\{d[\ln(I + I_{\text{si}})]/dV\}^{-1}} \times 100\%, \quad (4)$$

which is illustrated in Fig. 3(a) and Table III. It can be seen that when the bias voltage is fixed, the farther away the electron nonextensive parameter is from 1, the influence degree increases in a direct proportion.

C. Electron nonextensive parameter

Therefore, we adopt WDFM by using the form of Eq. (1). First, we analyze the statistics SSE and R^2 [see Figs. 3(b) and 3(c)] and then give the optimal value of the electron nonextensive parameter of 0.775 (see Table I), which is a quantity that cannot be measured with a traditional single probe. Then T_e can be determined (in fact T_e , Φ_p , and n_e can be determined at the same time), and the electron temperature measured by the nonextensive single electric probe (2.8358 eV, see Table I) is better than that measured by the traditional single probe (6.8843 eV, see Table I), which can be obtained from the analysis of I - V experimental data by using the nonextensive probe theory and the traditional probe theory respectively: The nonextensive single electric probe goodness-of-fit value $SSE = 303.9174$ arb. units is less than the traditional single probe goodness-of-fit value $SSE = 313.2270$ arb. units (see Table I).

D. Plasma potential

With the purpose of making use of the above theory under the nonextensive statistical framework to measure the plasma potential, from Eq. (1), letting $V = \Phi_f$ and $I = 0$, one can derive

$$\Phi_p = \Phi_f + \alpha_{q_{Fe}} T_e, \quad (5)$$

where if the unit of T_e is eV, then

$$\alpha_{q_{Fe}} = \left[\ln_{q_{Fe}} \left(\frac{A_q}{q_{Fe}} \sqrt{\frac{m_i}{2\pi m_e}} \right) + \frac{1}{2} \right] \left[\frac{A_q}{q_{Fe}} \sqrt{\frac{m_i}{2\pi m_e}} \right]^{1-q_{Fe}}, \quad (6)$$

is the sheath potential coefficient under the nonextensive statistical framework [see Fig. 2(d) and Table II]. It can be seen

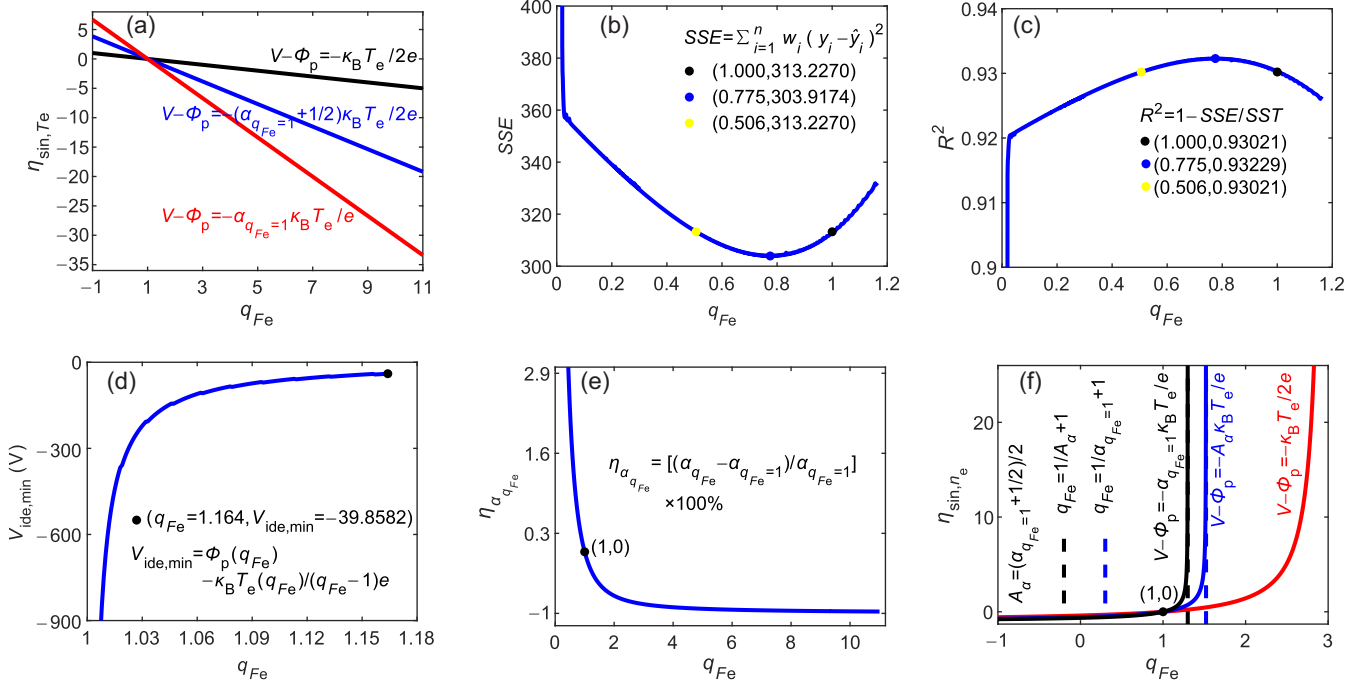


FIG. 3. Diagrams of three kinds of theoretical errors, two kinds of goodness of fit, and the maximum electron nonextensive parameter. (a) The error of the electron temperature measured by nonextensive single electric probe compared with that measured by traditional single probe decreases monotonically with respect to electron nonextensive parameter. (b) The variation curve of SSE with the electron nonextensive parameter shows that SSE reaches the minimum value when $q_{Fe} = 0.775$. (c) The variation curve of coefficient of determination (R^2) with electron nonextensive parameter shows that R^2 reaches the maximum value when $q_{Fe} = 0.775$. (d) The minimum bias voltage of the experimental data [22] determines the maximum allowable electron nonextensive parameter of 1.164. (e) In the range of interest, the error of the sheath potential coefficient measured by nonextensive single electric probe compared with that by the traditional single probe decreases with the increase of the electron nonextensive parameter. (f) The error curve of the electron density measured by a nonextensive single electric probe compared with that by a traditional single probe increases monotonically. For details see the supplementary information for the caption to Fig. 3. and Tables II–IV given in Appendix B.

from Eq. (5) that after measuring the floating potential and electron temperature and obtaining the sheath potential coefficient, the plasma potential in the case of extensive limit can be obtained: $\Phi_p(q_{Fe} = 1) = \Phi_f + \alpha_{q_{Fe}=1} T_e(q_{Fe} = 1)$, which proves the correctness of the proposed theory. However, we found that for the more general nonextensive case, the nonextensive parameter has an effect on the sheath potential coefficient, and the influence degree can be described by the following expression (method error):

$$\eta_{\alpha_{q_{Fe}}} = \frac{\alpha_{q_{Fe}} - \alpha_{q_{Fe}=1}}{\alpha_{q_{Fe}=1}} \times 100\%, \quad (7)$$

which is illustrated in Fig. 3(e) and Table II. It can be seen that when the electron nonextensive parameter is greater than 0 in the range we are interested in, with the increase of the electron nonextensive parameter, the nonextensive sheath potential coefficient has a complex nonlinear dependence of nonproportional decline. Therefore, the plasma potential determined by Eq. (5) which depends on floating potential, sheath potential coefficient, and electron temperature, which all depend on the electron nonextensive parameter, shows a complex dependence on the electron nonextensive parameter. Moreover, the plasma potential measured by the nonextensive single electric probe (19.4528 V, see Table I) is better than that measured by the traditional single probe (24.7228 V, see

Table I), which can also be obtained from the analysis of I - V experimental data by using the nonextensive probe theory and the traditional probe theory, respectively: The goodness-of-fit value of the nonextensive single electric probe $SSE = 303.9174$ arb. units is smaller than that of the traditional single probe $SSE = 313.2270$ arb. units (see Table I).

E. Electron density

In order to measure the electron density of plasma using the above theory under the nonextensive statistical framework, from Eq. (1) one can derive

$$n_{e,\text{sin}} = \frac{|I_{\text{si}}|}{eA_p \left(\frac{k_B T_{e,\text{sin}}}{m_i} \right)^{1/2} \left[1 - (q_{Fe} - 1) \frac{1}{2} \right]^{q_{Fe}-1 + \frac{1}{2}}}. \quad (8)$$

In the case of extensive limit, only $T_e(q_{Fe} = 1)$ is required to obtain the electron density $n_e(q_{Fe} = 1)$, namely it can reproduce the results under Maxwellian distribution, which proves the correctness of the proposed theory. However, for the more general nonextensive case, we find that the nonextensive parameters have an influence on the measurement of plasma density, and the influence degree can be described by

TABLE IV. Data presentation for curve of $\eta_{\text{sin},n_e} - q_{Fe}$ at $V - \Phi_p = -\kappa_B T_e / 2e$.

η_{sin,n_e}	$q_{Fe}(q_{Fe} < 1)$	$q_{Fe}(q_{Fe} \geq 1)$
$ \eta_{\text{sin},n_e} \leq 5\%$	$0.916 \leq q_{Fe} < 1.000$	$1.000 \leq q_{Fe} \leq 1.076$
$5\% < \eta_{\text{sin},n_e} \leq 10\%$	$0.823 \leq q_{Fe} < 0.916$	$1.076 < q_{Fe} \leq 1.147$
$10\% < \eta_{\text{sin},n_e} \leq 15\%$	$0.721 \leq q_{Fe} < 0.823$	$1.147 < q_{Fe} \leq 1.210$
$15\% < \eta_{\text{sin},n_e} \leq 20\%$	$0.606 \leq q_{Fe} < 0.721$	$1.210 < q_{Fe} \leq 1.270$
$20\% < \eta_{\text{sin},n_e} \leq 25\%$	$0.478 \leq q_{Fe} < 0.606$	$1.270 < q_{Fe} \leq 1.325$
$25\% < \eta_{\text{sin},n_e} \leq 30\%$	$0.332 \leq q_{Fe} < 0.478$	$1.325 < q_{Fe} \leq 1.376$
$30\% < \eta_{\text{sin},n_e} \leq 35\%$	$0.165 \leq q_{Fe} < 0.332$	$1.376 < q_{Fe} \leq 1.424$
$35\% < \eta_{\text{sin},n_e} \leq 40\%$	$-0.027 \leq q_{Fe} < 0.165$	$1.424 < q_{Fe} \leq 1.469$
$40\% < \eta_{\text{sin},n_e} \leq 45\%$	$-0.252 \leq q_{Fe} < -0.027$	$1.469 < q_{Fe} \leq 1.510$
$45\% < \eta_{\text{sin},n_e} \leq 50\%$	$-0.519 \leq q_{Fe} < -0.252$	$1.510 < q_{Fe} \leq 1.550$

the following expression (method error):

$$\eta_{\text{sin},n_e} = \left\{ \frac{\exp\left(-\frac{1}{2}\right)}{\sqrt{\eta_{\text{sin},T_e} + 1} \left[1 - (q_{Fe} - 1)^{\frac{1}{2}}\right]^{\frac{1}{q_{Fe} - 1} + \frac{1}{2}}} - 1 \right\} \times 100\%, \quad (9)$$

which is illustrated in Fig. 3(f) and Table IV. As you can see, when the electron nonextensive parameter is greater than -1 , with the increase of electron nonextensive parameter, method error of the electron density measured by nonextensive single electric probe compared with electron density measured by the traditional single probe has a complex nonlinear dependence of nonproportional rise on electron nonextensive parameter, namely plasma electron density determined by Eq. (8) has a complex nonlinear dependence of nonproportional rise on electron nonextensive parameter. In addition, the electron density of plasma measured by the nonextensive single electric probe ($1.936 \times 10^{15} \text{ cm}^{-3}$, see Table I) is better than that measured by the traditional single probe ($1.263 \times 10^{15} \text{ cm}^{-3}$, see Table I), which can also be obtained from the analysis of I - V experimental data by using the nonextensive probe theory and the traditional probe theory, respectively: The goodness-of-fit value of the nonextensive single electric probe $\text{SSE} = 303.9174$ arb. units is less than the traditional single probe goodness-of-fit value $\text{SSE} = 313.2270$ arb. units (see Table I).

In summary, using the proposed theory of nonextensive single electric probe, we measured the electron nonextensive parameter of 0.775 (see Table I) that cannot be measured by traditional electric probes and improved the measurement accuracy of the single electric probe: From the comprehensive effect diagram Fig. 4, it can be seen that the fitting method (NSP fitting and ESP fitting) is obviously superior to the formula method (ESP formula), and the nonextensive fitting method (NSP fitting) is superior to the traditional extensive fitting method (ESP fitting), which can be seen from that the nonextensive single electric probe goodness-of-fit value $\text{SSE} = 303.9174$ arb. units is smaller than the traditional single probe goodness-of-fit value $\text{SSE} = 313.2270$ arb. units, as shown in Table I.

IV. DISCUSSION AND CONCLUSION

Our results show a strong superiority in describing the plasma by replacing the Boltzmann-Gibbs statistical mechan-

ics with nonextensive statistical mechanics. The nonextensive single electric probe theory we established by introducing nonextensive statistical mechanics to account for the nonextensivity (possibly caused by long-range interactions [4]) of systems that have been proven by a large number of facts [6,7,11,12,23–38] not only obtained all the results of the traditional single probe at the extensive limit, which proves the correctness of the proposed theory, but also can measure electron nonextensive parameter (0.775, see Table I) that cannot be measured by the traditional electric probe and improve

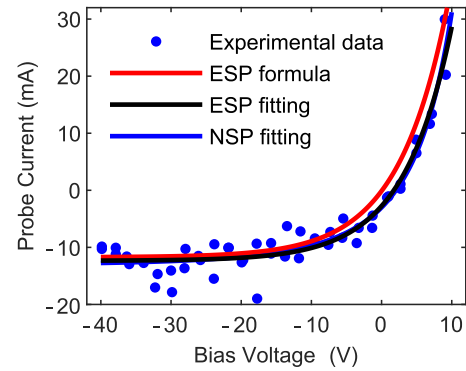


FIG. 4. Comprehensive effect diagram of processing single electric probe I - V experimental data with three methods. The blue points are 50 single probe I - V experimental data points [22] which are all the data points of $V \leq \Phi_s$. The red line is the intuitive curve corresponding to the results measured by the traditional (extensive) single probe formula (ESP formula), the black line is the intuitive curve corresponding to the single probe measurement results obtained by nonlinear fitting under the assumption that the plasma compositions satisfy the Maxwellian (extensive) distribution (ESP fitting), and the blue line is the intuitive curve corresponding to the single probe measurement results obtained by nonlinear fitting under the assumption that the plasma compositions satisfy the nonextensive distribution (NSP fitting) (for measurement results see Table I). From the figure, it is easy to see that the proximity of the red line to the experimental data points is worse than that of the black line and the blue line, and the blue line is better than the black line, which can be known from the comparison of the SSE and the coefficient of determination (R^2) [see Figs. 3(b) and 3(c), and Table I; for details see the supplementary information for the caption to Fig. 4 given in Appendix B].

the measurement accuracy of single electric probe, as shown in Table I.

Our work fills the gap where plasma cannot be described by Boltzmann-Gibbs statistical mechanics but can be described by nonextensive statistical mechanics while the corresponding electric probe theory and techniques are still lacking.

Our research is the starting point for nonextensive electric probe studies, and extensions to probes with magnetic fields, dual probes, triple probes, N probes, or probe arrays are being addressed.

ACKNOWLEDGMENTS

This work was supported by the Natural Science Foundation of Jiangxi Province (Grant No. 20181BAB211010), National Natural Science Foundation of China (Grants No. 11847023 and No. 11863004), International Science and Technology Cooperation Program of China (Grant No. 2015DFA61800), Jiangxi Province Key Laboratory of Fusion and Information Control (Grant No. 20171BCD40005), Innovation Credit Research Training Program of Nanchang University (Grants No. 55001808, No. 55001911, and No. 55001912), and College Students' Innovative Entrepreneurial Training Plan Program of Nanchang University (Grant No. 20190402214). We thank the anonymous reviewer for reminding constraint of the second law of thermodynamics.

APPENDIX A: FORMULA OF PROBE COLLECTING CURRENT

When the probe potential is less than the potential at ion sheath edge, namely $V < \Phi_p - (\kappa_B T_e / 2e)$, a sheath of positive charges will form around the probe. Current collected by probe is the current formed by the random thermal movement of charged particles entering the sheath. Under the framework of nonextensive statistics [17], adopting the one-dimensional nonextensive distribution function (Eq. (1) in Ref. [17]) and the similar derivation in Ref. [22], one finds that electron current I_e is the random thermal motion current multiplied by the nonextensive exponential factor (replace the Boltzmann factor [22]):

$$I_e = \frac{1}{4} en_e A_p \bar{v}_{q_{F_e}} \left[1 + (q_{F_e} - 1) \frac{e(V - \Phi_p)}{\kappa_B T_e} \right]^{\frac{1}{q_{F_e} - 1} + \frac{1}{2}}, \quad (\text{A1})$$

where Φ_p is plasma potential, κ_B is Boltzmann constant, e is electron charge, T_{rme} is electron temperature, n_e is electron density in undisturbed region, A_p is probe area, $\bar{v}_{q_{F_e}} = \frac{A_q}{q_{F_e}} \sqrt{\frac{8\kappa_B T_e}{\pi m_e}}$ is average thermal velocity of electron in nonextensive plasma, q_{F_e} is nonextensive parameter in electron distribution function of plasma, and A_q is normalization constant of nonextensive distribution. For collection of ion, according to Bohm's sheath formation theory [39], there is a presheath region outside the sheath, and ions flowing to the probe accelerate from undisturbed plasma region through the presheath region and reach the ion sound velocity $c_s (= \sqrt{\kappa_B T_e / m_i})$ at the edge of the sheath. What the probe surface collects is a current of ions across the edge of a sheath, called ion saturation current $I_{si} (= -|I_{si}|)$. Extending Bohm's sheath formation

theory [22,39] to nonextensive case, one has

$$|I_{si}| = e A_s n_e \left[1 - (q_{F_e} - 1) \frac{1}{2} \right]^{\frac{1}{q_{F_e} - 1} + \frac{1}{2}} \left(\frac{\kappa_B T_e}{m_i} \right)^{1/2}, \quad (\text{A2})$$

where A_s is the sheath area and $A_s \cong A_p$ when the shell thickness is negligible. Therefore, at this time, the total current collected by probe is

$$I = en_e A_p \sqrt{\frac{\kappa_B T_e}{m_i}} \left\{ \begin{aligned} & \frac{A_q}{q_{F_e}} \sqrt{\frac{m_i}{2\pi m_e}} \\ & \times \left[1 + (q_{F_e} - 1) \frac{e(V - \Phi_p)}{\kappa_B T_e} \right]^{\frac{1}{q_{F_e} - 1} + \frac{1}{2}} \\ & - \left[1 - (q_{F_e} - 1) \frac{1}{2} \right]^{\frac{1}{q_{F_e} - 1} + \frac{1}{2}} \end{aligned} \right\}. \quad (\text{A3})$$

The above analysis is based on the following assumptions:

- (i) No magnetic field;
- (ii) The plasma is thin, so the average free path of electrons and ions is much larger than the probe size (collision-free approximation);
- (iii) The electrons obey the nonextensive distribution, and the ion temperature is very low ($T_i \approx 0$, cold plasma approximation);
- (iv) The thickness of the formed sheath is much smaller than the probe size (order of several Debye length λ_D), thus allowing the use of plate approximation rather than relying on the geometry of the probe [22];
- (v) The emission of the secondary electron on the surface of the probe can be ignored, and the charged particles that hit on the probe do not react with the probe, namely the probe is an ideal absorber of charged particles.

APPENDIX B: SUPPLEMENTARY INFORMATION FOR FIGURES AND TABLES

1. Supplementary information for the caption to Fig. 1

The horizontal thick black line represents the single probe, which is wrapped by shorter insulation holder typically made of ceramic, quartz, or glass. The right end of the probe passes through the window through the vacuum chamber wall drawn by two parallel solid black lines and thin slashes and directly contacts the plasma represented by random scatter points. The left end of the probe is connected with the probe circuit, and the variable power supply with the positive pole upward is connected with the ammeter, which measures current collected by the probe (the positive direction of the current is set as the direction of flow from the probe surface to the plasma; it can be seen from the direction of charge movement of the electron current and ion current that the electron current is in the positive direction and the ion current is in the negative direction). A voltmeter connected to the grounded vacuum chamber wall measures a variable bias voltage applied to a single probe. By adjusting the bias voltage of the power supply, the current data collected by the probe under different bias voltage can be obtained.

2. Supplementary information for the caption to Fig. 2(a)

The abscissa is external changing bias voltage V applied to single probe, the range chose here is $[\Phi_p - 10\kappa_B T_e / e, \Phi_s]$, where Φ_s is potential at ion sheath edge, the surface of the probe begins to form an ion sheath when the applied bias

voltage on the single probe is reduced to Φ_s . The reason we do not care about the voltage ranged $V > \Phi_s$ is that the current collected by probe I has a jump when $V = \Phi_s$. Furthermore, the electron saturation flow obtained in the specific experiment is often not saturated, thus it is difficult to obtain plasma parameters by the electron saturation flow [40]; $\Phi_p - 10\kappa_B T_e/e \ll \Phi_p$ belongs to ion saturation current range. Actually, when $V \leq \Phi_p - 5\kappa_B T_e/e$ most of the electrons are rejected by the surface of the probe. The ordinate is the current collected by the probe (in our discussion, current being drawn by the probe is designated as positive) with range of $[I_{si}, I_s]$ in this work, where I_s is the current collected by the probe when variable bias voltage applied to the single probe is Φ_s , and I_{si} is ion saturation current, which corresponds to a negative bias potential with a large absolute value. The three curves in the figure are nonextensive single electric probe I - V characteristic curves when the electron nonextensive parameters q_{Fe} are respectively 0.8, 1, and 1.1. Focusing on the features common to the three curves first, the curve begins to increase monotonically as the probe bias voltage increases from a large negative value; furthermore, the speed of the monotonically increase is getting faster and faster, and there is a floating potential point ($\Phi_f, 0$) in the process of the probe bias voltage increase. This phenomenon can be interpreted mathematically as the expression of current collected by the probe has the derivative and second derivative larger than zero and the zero-point theorems for continuous function. Physically, the current collected by probe is the sum of electron current and ion current, and during the process of probe bias voltage increasing the electric field around the probe weaken the suppression of the electron current in the positive direction and gradually increases the suppression of the ion current in the opposite direction, which results in the increase of the current collected by the probe I ; since the electron mass m_e is much smaller than the ion mass m_i , the absolute value of the electron current is significantly larger than the absolute value of the ion saturation current; moreover, the absolute increase effect of the bias voltage on the electron current is more obvious than that on ion current, so that the increase of the current collected by probe is faster and faster. It is easy to find a point where the electron current is equal to the ion current during the growth process, which leads to the zero current collected by probe. For situations of different nonextensive parameters, when the nonextensive parameter is equal to 1, all conclusions for nonextensive case return to results under the Boltzmann-Gibbs statistical framework [17]; there is no an integral monotonicity, but we can discuss the local monotonicity with three derivative diagrams [see Figs. 2(b)–2(d)]: $g(q_{Fe}) - q_{Fe}$, $I_s - q_{Fe}$ and $\Phi_f - q_{Fe}$ (turn to discussion of $\alpha_{q_{Fe}} - q_{Fe}$).

3. Supplementary information for the caption to Fig. 2(b)

The abscissa is the electron nonextensive parameter q_{Fe} with range of $(-1, +\infty)$ [7,14,17,41,42], but when $q_{Fe} > 3$, an imaginary part of $g(q_{Fe})$ appears, and thus here the range takes $(-1, 3]$. It is worth noting that if one takes into account constraint of the second law of thermodynamics [43], then the range is reduced to $(0, 3]$ which is the same as that illustrated in Fig. 2(c); $q_{Fe}=1$ is the extensive limit, and at this point, all the conclusions go back to the results under

the Boltzmann-Gibbs statistical framework [17]. The ordinate is ion saturation current factor $g(q_{Fe})$ with range of $[-1, 0]$, and it shows the relative size of ion saturation current; when the ion saturation current factor $g(q_{Fe}) = -1$, ion saturation current takes minimum value (the largest absolute value). When the ion saturation current factor $g(q_{Fe})=0$, the ion saturation current is 0. It is easy to see that the dependence of ion saturation current factor on the electron nonextensive parameter has a monotone increasing trend. The mathematical reason is that the first derivative of ion saturation current factor $g(q_{Fe})$ with respect to the electron nonextensive parameter q_{Fe} is always greater than zero. Physically, the reason can be understood as that the proportion of high-energy electrons decreases gradually in the process of increasing the electron nonextensive parameter. Because the plasma in the undisturbed region satisfies the quasineutral condition, the proportion of the corresponding ions decreases gradually, and the speeds of ions' movement decrease as a whole, which leads to the decrease of the absolute value of ion saturation current.

4. Supplementary information for the caption to Fig. 2(c)

The range of abscissa, the electron nonextensive parameter, here is $(0, 3]$, because the current factor is negative when $q_{Fe} < 0$ and imaginary when $q_{Fe} > 3$ as well as positive and negative infinity when $q_{Fe} = 0$; $q_{Fe} = 1$ is the extent limit, the results in this case return to the results under Boltzmann-Gibbs statistical framework [17]. The ordinate is the total current factor with range of $[0, +\infty)$. Note that $h(q_{Fe}=1) = \sqrt{m_i/2\pi m_e} \exp(-1/2) - \exp(-1/2)$, namely at the extent limit, the total current collected by the nonextensive single electric probe is the same as the total current measured with the traditional single probe, which proves the correctness of the nonextensive single electric probe theory proposed in this work at the extent limit. The curve of total current factor measured by the nonextensive single electric probe is monotonically decreased with the increasing electron nonextensive parameter. When $q_{Fe} \in (0, 1]$, $h(q_{Fe})$ reaches the maximum at $q_{Fe} \rightarrow 0^+$ and then monotonically decreases with the increase of electron nonextensive parameter, but is still larger than $h(q_{Fe}=1) = \sqrt{m_i/2\pi m_e} \exp(-1/2) - \exp(-1/2)$ until $q_{Fe}=1$. When $q_{Fe} \in (1, 3]$, $h(q_{Fe})$ still monotonically decreases with the increase of the electron nonextensive parameter, less than $h(q_{Fe}=1) = \sqrt{m_i/2\pi m_e} \exp(-1/2) - \exp(-1/2)$, and reaches minimum value zero at $q_{Fe}=3$. The mathematical reason for this trend is that the first derivative of the total current factor to the electron nonextensive parameter is less than zero. The physical reasons are as follows: With the electron nonextensive parameter increasing, there are more and more low-speed electrons, and fewer and fewer high-energy electrons, so the temperature is getting lower and lower until the temperature is zero; in this process, the velocity of charged particles such as electrons and ions is getting smaller and smaller, namely current collected by probe is getting smaller and smaller, and when the temperature is zero, the electrons and ions, etc., do not move, so the corresponding particle flux is zero, and surely the total current collected by the probe is zero.

5. Supplementary information for the caption to Fig. 2(d)

The abscissa is electron nonextensive parameter with range of $[0, 11]$ here, because $\alpha_{q_{F_e}}$ has an imaginary part when $q_{F_e} < 0$, and the range of too-large parameter is not the range of experimental parameter; $q_{F_e} = 1$ is the extensive limit, and the results in this case all return to the results under the Boltzmann-Gibbs statistical framework [17]. The ordinate is nonextensive sheath potential coefficient with range of $(0.1000, +\infty)$ here; note that $\alpha_{q_{F_e}=1} = 3.3388$; that is, at the extensive limit, the sheath potential coefficient measured by nonextensive single electric probe is the same as measured by traditional single probe, which proves the correctness of proposed nonextensive single electric probe theory at the extensive limit. When $q_{F_e} > 0$, the curve of the nonextensive sheath potential coefficient with respect to electron nonextensive parameter is monotonically decreasing in the range of our interest. In the case of $q_{F_e} \in (0, 1)$, $\alpha_{q_{F_e}}$ approaches positive infinity when $q_{F_e} \rightarrow 0^+$ and then monotonically decreases with the increase of the electron nonextensive parameter but greater than $\alpha_{q_{F_e}=1}$, until $q_{F_e} = 1$ the value is $\alpha_{q_{F_e}=1} = 3.3388$; when $q_{F_e} \in (1, 11)$, $\alpha_{q_{F_e}}$ still monotonously decreases with the increase of electron nonextensive parameter but less than $\alpha_{q_{F_e}=1}$, until $q_{F_e} = 11$ the minimum value of 0.1000 is obtained. The mathematical reason for this change is that $d\alpha_{q_{F_e}}/dq_{F_e} < 0$ when $q_{F_e} \in (0, 11)$. Physically, in general, as the electron nonextensive parameter increases, the sheath potential coefficient decreases from positive infinity to 0.1000. Specifically, when $q_{F_e} \in (0, 1)$, the sheath potential coefficient measured by nonextensive single electric probe is larger than that measured by traditional single probe and approaches the maximum (positive infinity) when $q_{F_e} \rightarrow 0^+$; as the electron nonextensive parameter increases, the sheath potential coefficient becomes smaller and smaller. until $q_{F_e} = 1$ the sheath potential coefficient is $\alpha_{q_{F_e}=1} = 3.3388$, which is the same as the sheath potential coefficient measured by traditional single probe, because the nonextensive statistical mechanics is reduced to Boltzmann-Gibbs statistical mechanics; that is, at this time, the sheath potential coefficient is measured by the same method, thus the measured quantity values are naturally the same at this time. When $q_{F_e} \in (1, 11)$, the sheath potential coefficient measured by nonextensive single electric probe is smaller than that measured by traditional single probe, and as the electron nonextensive parameter increases, the small degree gradually increases from zero and finally reaches the maximum at $q_{F_e} = 11$, at which time the sheath potential coefficient drops to the minimum of 0.1000. The physical reason for this change is that as electron nonextensive parameters increase, there are more and more low-speed electrons and, at the same time, fewer and fewer high-energy electrons, so the temperature is getting lower and lower. In this process, the moving speed of charged particles such as electrons and ions is getting smaller and smaller, and the dropping of the sheath potential is more and more difficult; that is, the sheath potential coefficient is getting smaller and smaller.

6. Supplementary information for the caption to Fig. 3(a)

The ordinate is the error of the electron temperature measured by nonextensive single electric probe compared to the electron temperature measured by traditional single probe [see

Eq. (4) in text]; since it depends on the bias voltage, its value range is a function of the bias voltage, and the specific value is uncertain, but the typical value is shown in the corresponding table (Table III); note that $\eta_{\text{sin}, T_e}(q_{F_e} = 1) = 0$, namely at the extensive limit, the electron temperature measured by the nonextensive single electric probe is equal to that obtained by traditional single probe, which proves the correctness of the proposed nonextensive single electric probe theory at the extensive limit. The curves for the error of the electron temperature measured by nonextensive single electric probe compared to the electron temperature measured by traditional single probe is monotonically decreasing with the increasing electron nonextensive parameter. When $q_{F_e} \in (-1, 1]$, η_{sin, T_e} reaches the maximum at $q_{F_e} \rightarrow -1$, and then η_{sin, T_e} is monotonically decreasing with the increasing electron nonextensive parameter, and η_{sin, T_e} is always greater than zero in the process until $q_{F_e} = 1$, $\eta_{\text{sin}, T_e} = 0$; η_{sin, T_e} is still monotonically decreasing with the increasing electron nonextensive parameter when $q_{F_e} \in (1, +\infty)$, and η_{sin, T_e} is less than zero until $q_{F_e} = +\infty$, and η_{sin, T_e} reaches negative infinity at this time. The mathematical reason for this trend is $d\eta_{\text{sin}, T_e}/dq_{F_e} < 0$. Physically, in general, as the electron nonextensive parameter increases, the error decreases from positive to negative. Specifically, the electron temperature measured by the nonextensive single electric probe is larger than the electron temperature measured by the traditional single probe, and the maximum of the error is $\eta_{\text{sin}, T_e}(q_{F_e} \rightarrow -1) = -2(V - \Phi_p)/\{d[\ln(I + I_{\text{si}})]/dV\}^{-1} \times 100\%$, and the error is getting smaller and smaller with the increasing electron nonextensive parameter until $q_{F_e} = 1$ the error disappeared, because nonextensive statistical mechanics is reduced to Boltzmann-Gibbs statistical mechanics at this time, namely the temperature is obtained by the same way, where surely the error is equal to zero. When $q_{F_e} \in (1, +\infty)$, the electron temperature measured by nonextensive single electric probe is smaller than that of the traditional single probe; actually, the gap gradually increases from zero and reaches the maximum value $\eta_{\text{sin}, T_e}(q_{F_e} \rightarrow +\infty) = -\infty$. Namely the electron temperature measured by the nonextensive single electric probe is zero at this time. The physical reason for this trend is that as the electron nonextensive parameter increases, there are more low-speed electrons and fewer high-energy electrons, so the temperature is getting lower and lower until the temperature is zero.

7. Supplementary information for the caption to Fig. 3(b)

The range of abscissa, the electron nonextensive parameter, here is $[0, 1.164]$; the reason for not considering the situation of $-1 < q_{F_e} < 0$ is that when $q_{F_e} < 0$, the total current factor is negative [see Fig. 2(c)] and the imaginary part of $\alpha_{q_{F_e}}$ appears [see Fig. 2(d)]. The maximum value of the electron nonextensive parameter $q_{F_e, \text{max}} = \text{Solution_of}\{V_{\text{min}} = \Phi_p - \frac{1}{q_{F_e}-1} \frac{\kappa_B T_e}{e}\}$, which shows that the range of electron nonextensive parameters that the nonextensive single electric probe can deal with also depends on the minimum bias voltage value of the I - V experimental data [22], which here is $q_{F_e, \text{max}} = 1.164$ [see Fig. 3(d)]; $q_{F_e} = 1$ is the extensive limit, and the results in this case all return to the results under the Boltzmann-Gibbs statistical framework [17]. The ordinate is SSE with a range of $[303.9174, 4537.5306]$ arb.

units; note that $SSE(q_{Fe} = 1) = 313.2270$ arb. units, namely at the extensive limit, the nonlinear fitting SSE obtained by using the nonextensive single electric probe theory is the same as that obtained by the traditional single probe theory, which proves the correctness of the proposed nonextensive single electric probe theory at the extensive limit. The curve of the nonlinear fitting SSE obtained by using the nonextensive single electric probe theory decreases first and then increases with the increasing electron nonextensive parameter, namely the nonextensive fitting effect becomes better first and then worse (there are fluctuations in very few places). Specifically, when $q_{Fe} \rightarrow 0$, the maximum SSE of nonlinear fitting can be obtained, $SSE(q_{Fe} \rightarrow 0) = 4537.5306$ arb. units; when $q_{Fe} \in (0, 0.506)$, with the increase of electron nonextensive parameter, the SSE of nonlinear fitting becomes smaller and smaller (there are fluctuations in very few places) but is larger than the SSE of nonlinear fitting obtained by using the traditional single probe theory, until $q_{Fe} = 0.506$ it is equal to the nonlinear fitting SSE = 313.2270 arb. units obtained by using the traditional single probe theory; when $q_{Fe} \in (0.506, 0.775)$, the SSE of nonlinear fitting obtained by using the nonextensive single electric probe theory still decreases with the increase of the electron nonextensive parameter, until $q_{Fe} = 0.775$ the SSE of nonlinear fitting reaches the minimum of 303.9174 arb. units; that is, the fitting result is closest to the real value at this time. After that, the SSE of nonlinear fitting increases with the increase of electron nonextensive parameter but is still smaller than the SSE of nonlinear fitting obtained by using the traditional single probe theory; until $q_{Fe} = 1$, nonlinear fitting SSE is the same as that obtained by using the traditional single probe theory, because the nonextensive statistical mechanics is reduced to Boltzmann-Gibbs statistical mechanics, namely, the same theory is used at this time, and the 2 SSEs are naturally the same. When $q_{Fe} \in (1, 1.164)$, the SSE of nonlinear fitting obtained by using the nonextensive single electric probe theory is larger than that obtained by using the traditional single probe theory, and with the increase of the electron nonextensive parameter, the large degree gradually increases from zero until the maximum electron nonextensive parameter $q_{Fe, \max} = 1.164$; at this point, $SSE(q_{Fe} = 1.164) = 332.0206$ arb. units. The mathematical reason for this trend is that the SSE of nonlinear fitting has been optimized once the electron nonextensive parameter q_{Fe} increase from 0, and until $q_{Fe} = 0.775$, the optimal value 303.9174 is obtained. After reaching the optimal value, the nonlinear fitting results have been getting worse with the increase of the nonextensive parameter. The physical reason for this change is that Boltzmann-Gibbs statistical mechanics is not an optimal statistical mechanics to describe the plasma system, but for the nonextensive statistical mechanics, because of its variable nonextensive parameter which can be adjusted, the theory can better describe the real plasma system. here, the real plasma system [22] is described by the nonextensive statistical mechanics with an electron nonextensive parameter of 0.775.

8. Supplementary information for the caption to Fig. 3(c)

The ordinate is the nonlinear fitting coefficient of determination R^2 with range of $[-0.2519, 0.93229]$ here; note that $R^2(q_{Fe} = 1) = 0.93021$; that is, at the extensive limit, nonlinear fitting coefficient of determination obtained

by nonextensive single electric probe theory is equal to that obtained by traditional single probe theory, which proves the correctness of the nonextensive single electric probe theory proposed in this work at the extensive limit. The curve of nonlinear fitting coefficient of determination obtained by the nonextensive single electric probe theory is increased first and then decreased with a monotonically increasing electron nonextensive parameter (fluctuations exist in very few places). Physically, in general, as electron nonextensive parameter increases from 0 to 0.775, the nonlinear fitting coefficient of determination is closer to 1, and then the fitting result is surely closer to reality. By contrast, as the electron nonextensive parameter increases further from 0.775, the farther the fitting result is from the real. Specifically, when $q_{Fe} \rightarrow 0$, the minimum value of nonlinear fitting coefficient of determination obtained by nonextensive single electric probe theory is $R^2(q_{Fe} \rightarrow 0) = -0.01098$; the nonlinear fitting coefficient of determination obtained by nonextensive single electric probe theory increases with the increase of the electron nonextensive parameter when $q_{Fe} \in (0, 0.506]$, but less than that obtained by traditional single probe theory, until $q_{Fe} = 0.506$ the nonlinear fitting coefficient of determination obtained by nonextensive electric single probe theory will be equal to that obtained by traditional single probe theory. As the electron nonextensive parameter increases from 0.506, the nonlinear fitting coefficient of determination is monotonically increasing until $q_{Fe} = 0.775$ (fluctuations exist in very few places) reaching the maximum coefficient of determination $R^2(q_{Fe} = 0.775) = 0.93229$; namely the nonlinear fitting coefficient of determination obtained by nonextensive single electric probe theory reaches the maximum value (closest to 1). In other words, it is the closest fitting result to the real; then, as the electron nonextensive parameter increases, the nonlinear fitting coefficient of determination decreases. The situation continues until $q_{Fe} = 1$. The nonlinear fitting coefficient of determination obtained by nonextensive single electric probe theory is equal to that obtained by traditional single probe theory, because nonextensive statistical mechanics is reduced to Boltzmann-Gibbs statistical mechanics at this time; that is, nonlinear fitting coefficients of determination are obtained by the same theory, and the coefficients of determination are surely the same. When $q_{Fe} \in (1, 1.164)$, the nonlinear fitting coefficient of determination obtained by nonextensive single electric probe theory is less than that obtained by traditional single probe theory; furthermore, as the electron nonextensive parameter increases, the degree of smallness is gradually increased from zero. Finally, the nonlinear fitting coefficient of determination reaches $R^2(q_{Fe} = 1.164) = 0.926024$ at the edge of electron nonextensive parameter $q_{Fe} = 1.164$. The reason for this change is that Boltzmann-Gibbs statistical mechanics is not the optimal statistical mechanics to describe plasma systems; by contrast, nonextensive statistical mechanics has the adjustable nonextensive parameters, so that the nonextensive statistical mechanics can better describe real plasma systems. The real plasma system [22] here is described by a nonextensive statistical mechanics with an electron nonextensive parameter of 0.775, and this is the same result [see Fig. 3(b)] as the fitting method measured by SSE for goodness of fit, which has confirmed the reliability of our fitting results.

9. Supplementary information for the caption to Fig. 3(d)

The range of abscissa, the electron nonextensive parameter, is $[1, +\infty)$ because for all the electron nonextensive parameters of $q_{Fe} < 1$ the ideal minimum voltage which can be described by the nonextensive single electric probe theory is negative infinite; $q_{Fe} = 1$ is the extensive limit, the results in this case return to the results under the Boltzmann-Gibbs statistical framework [17]. The ordinate is the ideal minimum voltage that can be described by the nonextensive single electric probe theory when the nonextensive parameter is greater than or equal to 1 with range of $(-\infty, -39.8582]$ V, where the minimum value of the bias voltage in the experimental data [22] is $V_{\text{ide},\min}(q_{Fe} = 1.164) = -39.8582$ V. Note that $V_{\text{ide},\min}(q_{Fe} \rightarrow 1) = -\infty$; that is, at the extensive limit, the ideal minimum voltage that can be described by the nonextensive single electric probe theory is negative infinity, returning to the result under the Boltzmann-Gibbs statistical framework, which proves the correctness of the proposed nonextensive single electric probe theory at the extensive limit. When the nonextensive parameter is greater than 1, the ideal minimum voltage described by the nonextensive single electric probe theory is monotonically increasing with the increase of the electron nonextensive parameter. When $q_{Fe} \in [1, +\infty)$, at $q_{Fe} = 1$, $V_{\text{ide},\min}$ reaches minimum value negative infinity, which is equal to the ideal minimum voltage described by traditional single probe theory, and then monotonically increases with the increase of nonextensive parameter until $q_{Fe} = 1.164$. At this point, the ideal minimum voltage described by nonextensive single electric probe theory is -39.8582 V, which is the same as the smallest single probe experimental bias voltage in the experimental data [22] we used. Physically, in general, when $q_{Fe} > 1$ the ideal minimum voltage that can be described by the nonextensive single electric probe theory increases with increasing electron nonextensive parameter. Specifically, at extensive limit, the ideal minimum voltage that can be described by the nonextensive single electric probe theory is negative infinity (minimum) which is equal to the ideal minimum voltage described by traditional single probe theory, because nonextensive statistical mechanics is reduced to Boltzmann-Gibbs statistical mechanics at this point; that is, the voltage is obtained by the same single probe theory, and surely the results are the same. When $q_{Fe} \in (1, +\infty)$, the ideal minimum voltage that can be described by the nonextensive single electric probe theory increases monotonically from negative infinity, although the increase speed gradually slows down later and reaches the maximum value of voltage -39.8582 V (the minimum bias voltage of the experimental data, too) at maximum electron nonextensive parameter 1.164. The physical reason for this change is that the range of electron nonextensive parameter that can be processed by nonextensive single electric probe depends on the minimum bias voltage of the experimental data; actually, the higher the minimum bias voltage, the larger the electron nonextensive parameter. Specifically, the relationship between the maximum value of the electron nonextensive parameter and the minimum bias voltage is $q_{Fe,\max} = \text{Solution_of}\{V_{\min} = \Phi_p - \frac{1}{q_{Fe}-1} \frac{k_B T_e}{e}\}$, which shows that the range (maximum) of the electron nonextensive parameter that can be processed by the nonextensive single electric probe theory depends on the minimum bias

voltage value of the I - V experimental data, and the higher the minimum bias voltage, the larger the maximum allowable electron nonextensive parameter is; $q_{Fe} = 1$ is the extensive limit, and at this point the results return to those under the Boltzmann-Gibbs statistical framework [17].

10. Supplementary information for the caption to Fig. 3(e)

The abscissa is electron nonextensive parameter with range of $[0, 11]$ here [see Fig. 2(d)]; $q_{Fe} = 1$ is the extensive limit, the results in this case return to the results under the Boltzmann-Gibbs statistical framework [17]. The ordinate $\eta_{\alpha_{q_{Fe}}}$ is the error of the sheath potential coefficient measured by nonextensive single electric probe compared with that by the traditional single probe with range of $[-0.9700, +\infty)$. Note that $\eta_{\alpha_{q_{Fe}}}(q_{Fe} = 1) = 0$; that is, at the extensive limit, the sheath potential coefficient measured by nonextensive single electric probe is the same as that measured by traditional single probe, which proves the correctness of proposed nonextensive single electric probe theory at the extensive limit. The curve for error of the sheath potential coefficient measured by nonextensive single electric probe compared with that by the traditional single probe with respect to electron nonextensive parameter is monotonically decreasing in the range of $[0, 11]$. Physically, with the increase of electron nonextensive parameter, the error of the sheath potential coefficient measured by nonextensive single electric probe compared with that by the traditional single probe decreases from the positive infinity in the range of $[0, 11]$, until $q_{Fe} = 11$ $\eta_{\alpha_{q_{Fe}}}$ takes the minimum of -0.9700 . The physical reason for this change is that as the electron nonextensive parameter increases, there are more and more low-speed electrons, and fewer and fewer high-energy electrons, so the temperature is getting lower and lower; in this process, the moving speed of charged particles such as electrons and ions is getting smaller and smaller, and the dropping of sheath potential is more and more difficult, namely the sheath potential coefficient is getting smaller and smaller.

11. Supplementary information for the caption to Fig. 3(f)

The abscissa is the electron nonextensive parameter because of the need to make sure η_{sin,n_e} is a real number (namely an imaginary part cannot appear); meanwhile the denominator cannot be zero, so there are limits of $\eta_{\text{sin},T_e} + 1 > 0$ and $[1 - (q_{Fe} - 1)^{\frac{1}{2}}] > 0$. The maximum value of q_{Fe} varies with different bias voltage, and the range of values can be regarded as $(-1, 1 - \{d[\ln(I + I_{si})]/dV\}^{-1}/(V - \Phi_p))$; $q_{Fe} = 1$ is the extensive limit, and in this case, the conclusions all go back to the results under the Boltzmann-Gibbs statistical framework [17]. In addition, when $q_{Fe} \rightarrow 1 - \{d[\ln(I + I_{si})]/dV\}^{-1}/(V - \Phi_p)$, the error $\eta_{\text{sin},n_e} \rightarrow +\infty$. The ordinate is the error of the electron density measured by a nonextensive single electric probe compared with that by a traditional single probe which is expressed by Eq. (9) with a range of $[\exp(-\frac{1}{2})/\sqrt{\eta_{\text{sin},T_e}(q_{Fe} = -1) + 1}, +\infty) = (\exp(-\frac{1}{2})/\sqrt{-2(V - \Phi_p)\{d[\ln(I + I_{si})]/dV\}^{-1} + 1}, +\infty)$, where the minimum value depends on the bias voltage. Note that $\eta_{\text{sin},n_e}(q_{Fe} = 1) = 0$, namely at the extensive limit, the electron density measured by nonextensive single electric

probe is the same as that measured by traditional single probe, which proves the correctness of the nonextensive single electric probe theory proposed in this work at the extensive limit. The curve for error of the electron density measured by a nonextensive single electric probe compared with that by a traditional single probe with the increase of the electron nonextensive parameter is monotonely increasing. When $q_{F_e} \in (-1, 1)$, η_{sin, T_e} takes minimum at $q_{F_e} \rightarrow -1$, and after that, it increases monotonously with the increase of electron nonextensive parameter but is less than zero, until $q_{F_e} = 1$, the value is zero; when $q_{F_e} \in (1, 1 - \{d[\ln(I + I_{\text{si}})]/dV\}^{-1}/(V - \Phi_p))$, η_{sin, T_e} still monotonically increases with the increase of the electron nonextensive parameter but is greater than zero, until $q_{F_e} \rightarrow 1 - \{d[\ln(I + I_{\text{si}})]/dV\}^{-1}/(V - \Phi_p)$, the value is $+\infty$. The mathematical reason is $d\eta_{\text{sin}, T_e}/dq_{F_e} > 0$. Physically, with the increase of electron nonextensive parameter, the error goes from negative to positive. When $q_{F_e} \in (-1, 1)$, the electron density measured by nonextensive single electric probe is smaller than that measured by traditional single probe, and the maximum error $\eta_{\text{sin}, T_e}(q_{F_e} \rightarrow -1) = [\exp(-\frac{1}{2})/\sqrt{\frac{-2(V - \Phi_p)}{\{d[\ln(I + I_{\text{si}})]/dV\}^{-1}} + 1} - 1] \times 100\%$. With the increase of the electron nonextensive parameter, the error becomes smaller and smaller; until $q_{F_e} = 1$, the error disappears, and at this time, the nonextensive statistical mechanics is reduced to Boltzmann-Gibbs statistical mechanics, so the error is naturally zero. When $q_{F_e} \in (1, +\infty)$, the electron density measured by the nonextensive single electric probe is larger than that measured by the traditional single probe, and with the increase of the electron nonextensive parameter, the large degree gradually increases from zero and finally reaches the maximum value of $+\infty$ when $q_{F_e} \rightarrow 1 - \{d[\ln(I + I_{\text{si}})]/dV\}^{-1}/(V - \Phi_p)$; that is, the electron density measured by the nonextensive single electric probe is infinite at this point. The physical reason for this change is that with the increase of the electron nonextensive parameter, the percentage of electrons at large speed decreases, while keeping the material flux constant (i.e., the current collected by probe constant), and the electron density must increase.

12. Supplementary information for the caption to Fig. 4

The abscissa is the external changing bias voltage with range of $[-39.8582, 9.1489]$ V applied to the single probe; actually, the minimum voltage in the experimental data is -39.8582 V, which determines the maximum value of the allowable electron nonextensive parameter 1.164 [see Fig. 3(d)], and the maximum voltage 9.1489 V ($\simeq \Phi_s$) is obtained by the method of “semilog-knee” [22]. The ordinate is total current collected by single probe with range of $[-18.98, 29.97]$ mA. Blue points are the I - V experimental data [22] used in this work, and we select all the data that meet the criteria $V \leq \Phi_s$, a total of 50 data points [22], and other data are not the processing object of the proposed theory. The red line is the intuitive curve corresponding to the results measured by method of the ESP formula, the black line is the intuitive curve corresponding to the single probe measurement results obtained by method of ESP fitting, and the blue line is the intuitive curve corresponding to the single probe measurement results obtained by method of NSP fitting (for measurement results see Table I). The three curves conform to the trend of the single probe measurement curve and always increase with the increase of the bias voltage when $V \leq \Phi_s$. It is easy to read from the figure that the red line; namely the result measured by the ESP formula method is the worst result of closing to the experimental data. We use the sum of squares due to error SSE and the coefficient of determination R^2 to determine which is the closest to the experimental data among the three curves. The calculations [see Figs. 3(b) and 3(c) and Table I] show that the result measured by the method of NSP fitting is closest to the I - V experimental data under the above two indexes, which proves the superiority of nonextensive statistical mechanics. It is worth mentioning that the nonextensivity of the system implied by the I - V experiment data can be reflected by the optimal electron nonextensive parameter given by the NSP fitting method based on nonextensive statistical mechanics, which is the most important function of the nonextensive single electric probe proposed in this work (as mentioned in the title), and the electron nonextensive parameter value we measured here is 0.775.

-
- [1] V. I. Demidov, S. V. Ratynskaia, and K. Rypdal, Electric probes for plasmas: The link between theory and instrument, *Rev. Sci. Instrum.* **73**, 3409 (2002).
- [2] V. A. Godyak, R. B. Piejak, and B. M. Alexandrovich, Probe diagnostics of non-Maxwellian plasmas, *J. Appl. Phys.* **73**, 3657 (1993).
- [3] D. Darian, S. Marholm, M. Mortensen, and W. J. Miloch, Theory and simulations of spherical and cylindrical Langmuir probes in non-Maxwellian plasmas, *Plasma Phys. Controlled Fusion* **61**, 085025 (2019).
- [4] C. Anteneodo and C. Tsallis, Breakdown of Exponential Sensitivity to Initial Conditions: Role of the Range of Interactions, *Phys. Rev. Lett.* **80**, 5313 (1998).
- [5] E. Cohen, Statistics and dynamics, *Physica A* **305**, 19 (2002).
- [6] G. Van Hoven, Observation of Plasma Oscillations, *Phys. Rev. Lett.* **17**, 169 (1966).
- [7] J. A. S. Lima, R. Silva, and J. Santos, Plasma oscillations and nonextensive statistics, *Phys. Rev. E* **61**, 3260 (2000).
- [8] J. M. Liu, J. S. De Groot, J. P. Matte, T. W. Johnston, and R. P. Drake, Measurements of Inverse Bremsstrahlung Absorption and Non-Maxwellian Electron Velocity Distributions, *Phys. Rev. Lett.* **72**, 2717 (1994).
- [9] G. Livadiotis and D. J. McComas, Invariant kappa distribution in space plasmas out of equilibrium, *Astrophys. J.* **741**, 88 (2011).
- [10] L. Sorriso-Valvo, F. Catapano, A. Retinò, O. Le Contel, D. Perrone, O. W. Roberts, J. T. Coburn, V. Panebianco, F. Valentini, S. Perri, A. Greco, F. Malara, V. Carbone, P. Veltri, O. Pezzi, F. Fraternali, F. Di Mare, R. Marino, B. Giles, T. E. Moore, C. T. Russell, R. B. Torbert, J. L. Burch, and Y. V. Khotyaintsev, Turbulence-Driven Ion Beams in the Magne-

- tospheric Kelvin-Helmholtz Instability, *Phys. Rev. Lett.* **122**, 035102 (2019).
- [11] C. Tsallis, *Introduction to Nonextensive Statistical Mechanics: Approaching a Complex World* (Springer, Berlin, 2009).
- [12] C. Tsallis, Nonextensive statistical mechanics and thermodynamics; see <http://tsallis.cat.cbpf.br/biblio.htm> for a regularly updated bibliography.
- [13] R. G. DeVoe, Power-Law Distributions for a Trapped Ion Interacting with a Classical Buffer Gas, *Phys. Rev. Lett.* **102**, 063001 (2009).
- [14] H.-B. Qiu, H.-Y. Song, and S.-B. Liu, Collisionless damping of geodesic acoustic mode in plasma with nonextensive distribution, *Phys. Plasmas* **21**, 062310 (2014).
- [15] R. A. Treumann and C. H. Jaroschek, Gibbsian Theory of Power-Law Distributions, *Phys. Rev. Lett.* **100**, 155005 (2008).
- [16] N. Oyama, H. Mizuno, and K. Saitoh, Avalanche Interpretation of the Power-Law Energy Spectrum in Three-Dimensional Dense Granular Flow, *Phys. Rev. Lett.* **122**, 188004 (2019).
- [17] H.-B. Qiu and S.-Q. Liu, Dispersion relation of longitudinal oscillation in relativistic plasmas with nonextensive distribution, *Phys. Plasmas* **25**, 102102 (2018).
- [18] T. S. Biró and A. Jakovác, Power-Law Tails from Multiplicative Noise, *Phys. Rev. Lett.* **94**, 132302 (2005).
- [19] G. Livadiotis and D. J. McComas, Beyond kappa distributions: Exploiting tsallis statistical mechanics in space plasmas, *J. Geophys. Res.: Space Phys.* **114**, A11105 (2009).
- [20] G. Livadiotis, Statistical background of kappa distributions: Connection with nonextensive statistical mechanics, in *Kappa Distributions*, edited by G. Livadiotis (Elsevier, Amsterdam, 2017), Chap. 1, pp. 3–63.
- [21] C. Tsallis, Possible generalization of Boltzmann-Gibbs statistics, *J. Stat. Phys.* **52**, 479 (1988).
- [22] B. Lipschultz, I. Hutchinson, B. LaBombard, and A. Wan, Electric probes in plasmas, *J. Vac. Sci. Technol. A* **4**, 1810 (1986).
- [23] P. H. Yoon, T. Rhee, and C.-M. Ryu, Self-Consistent Generation of Superthermal Electrons by Beam-Plasma Interaction, *Phys. Rev. Lett.* **95**, 215003 (2005).
- [24] B. Liu and J. Goree, Superdiffusion and Non-Gaussian Statistics in a Driven-Dissipative 2d Dusty Plasma, *Phys. Rev. Lett.* **100**, 055003 (2008).
- [25] P. Douglas, S. Bergamini, and F. Renzoni, Tunable Tsallis Distributions in Dissipative Optical Lattices, *Phys. Rev. Lett.* **96**, 110601 (2006).
- [26] E. Lutz and F. Renzoni, Beyond Boltzmann-Gibbs statistical mechanics in optical lattices, *Nat. Phys.* **9**, 615 (2013).
- [27] R. M. Pickup, R. Cywinski, C. Pappas, B. Farago, and P. Fouquet, Generalized Spin-Glass Relaxation, *Phys. Rev. Lett.* **102**, 097202 (2009).
- [28] V. Khachatryan, A. M. Sirunyan, A. Tumasyan, W. Adam, T. Bergauer, M. Dragicevic, J. Erö, C. Fabjan, M. Friedl, R. Frühwirth *et al.* (CMS Collaboration), Transverse-Momentum and Pseudorapidity Distributions of Charged Hadrons in pp collisions at $\sqrt{s} = 7\text{TeV}$, *Phys. Rev. Lett.* **105**, 022002 (2010).
- [29] S. Chatrchyan, V. Khachatryan, A. M. Sirunyan, A. Tumasyan, W. Adam, T. Bergauer, M. Dragicevic, J. Erö, C. Fabjan, M. Friedl *et al.* (CMS Collaboration), Search for new physics with jets and missing transverse momentum in pp collisions at $\sqrt{s} = 7\text{TeV}$, *J. High Energy Phys.* **08** (2011) 155.
- [30] K. Aamodt, N. Abel, U. Abeysekara, A. A. Quintana, A. Abramyan, D. Adamová, M. Aggarwal, G. A. Rinella, A. Agocs, S. A. Salazar *et al.* (ALICE Collaboration), Transverse momentum spectra of charged particles in proton-proton collisions at $\sqrt{s} = 900\text{GeV}$ with ALICE at the LHC, *Phys. Lett. B* **693**, 53 (2010).
- [31] B. Abelev, J. Adam, D. Adamová, A. M. Adare, M. M. Aggarwal, G. Aglieri Rinella, A. G. Agocs, A. Agostinelli, S. Aguilar Salazar, Z. Ahammed *et al.* (ALICE Collaboration), Measurement of electrons from semileptonic heavy-flavor hadron decays in pp collisions at $\sqrt{s} = 7\text{TeV}$, *Phys. Rev. D* **86**, 112007 (2012).
- [32] G. Aad, B. Abbott, J. Abdallah, A. A. Abdelalim, A. Abdesselam, O. Abidinov, B. Abi, M. Abolins, H. Abramowicz, H. Abreu *et al.* (ATLAS Collaboration), Charged-particle multiplicities in pp interactions measured with the ATLAS detector at the LHC, *New J. Phys.* **13**, 053033 (2011).
- [33] A. Adare, S. Afanasiev, C. Aidala, N. N. Ajitanand, Y. Akiba, H. Al-Bataineh, J. Alexander, K. Aoki, L. Aphecetche, R. Armendariz *et al.* (PHENIX Collaboration), Measurement of neutral mesons in $p + p$ collisions at $\sqrt{s} = 200\text{GeV}$ and scaling properties of hadron production, *Phys. Rev. D* **83**, 052004 (2011).
- [34] A. Adare, S. Afanasiev, C. Aidala, N. N. Ajitanand, Y. Akiba, H. Al-Bataineh, A. Al-Jamel, J. Alexander, A. Angerami, K. Aoki *et al.* (PHENIX Collaboration), Production of ω mesons in $p+p$, $d+\text{Au}$, $\text{Cu}+\text{Cu}$, and $\text{Au}+\text{Au}$ collisions at $\sqrt{s_{NN}} = 200\text{GeV}$, *Phys. Rev. C* **84**, 044902 (2011).
- [35] C.-Y. Wong and G. Wilk, Tsallis fits to p_T spectra and multiple hard scattering in pp collisions at the LHC, *Phys. Rev. D* **87**, 114007 (2013).
- [36] L. Marques, E. Andrade-II, and A. Deppman, Nonextensivity of hadronic systems, *Phys. Rev. D* **87**, 114022 (2013).
- [37] R. Aaij, B. Adeva, M. Adinolfi, A. Affolder, Z. Ajaltouni, S. Akar, J. Albrecht, F. Alessio, M. Alexander, S. Ali *et al.* (LHCb Collaboration), Study of the production of Λ_b^0 and \bar{B}^0 hadrons in pp collisions and first measurement of the $\Lambda_b^0 \rightarrow J/\psi p K^-$ branching fraction, *Chin. Phys. C* **40**, 011001 (2016).
- [38] G. Combe, V. Richefeu, M. Stasiak, and A. P. F. Atman, Experimental Validation of a Nonextensive Scaling Law in Confined Granular Media, *Phys. Rev. Lett.* **115**, 238301 (2015).
- [39] R. K. Wakerling and A. Guthrie, *The Characteristics of Electrical Discharges in Magnetic Fields*, National Nuclear Energy series, Div. I (McGraw-Hill, New York, 1949).
- [40] L. Wang, *Experimental Physics of Magnetic Confinement Plasmas* (Science Press, Beijing, 2018).
- [41] R. Silva, A. Plastino, and J. A. S. Lima, A Maxwellian path to the q-nonextensive velocity distribution function, *Phys. Lett. A* **249**, 401 (1998).
- [42] S. Q. Liu and H. B. Qiu, Dust acoustic instability with nonextensive distribution, *J. Plasma Phys.* **79**, 105 (2013).
- [43] J. A. S. Lima, R. Silva, and A. R. Plastino, Nonextensive Thermostatistics and the H Theorem, *Phys. Rev. Lett.* **86**, 2938 (2001).